Checking Safety of Neural Networks with SMT Solvers: a Comparative Evaluation. *

Luca Pulina and Armando Tacchella

DIST, Università di Genova, Viale Causa, 13 – 16145 Genova, Italy
Luca.Pulina@unige.it - Armando.Tacchella@unige.it

Abstract. In this paper we evaluate state-of-the-art SMT solvers on encodings of verification problems involving Multi-Layer Perceptrons (MLPs), a widely used type of neural network. Verification is a key technology to foster adoption of MLPs in safety-related applications, where stringent requirements about performance and robustness must be ensured and demonstrated. While safety problems for MLPs can be attacked solving Boolean combinations of linear arithmetic constraints, the generated encodings are hard for current state-of-the-art SMT solvers, limiting our ability to verify MLPs in practice.

1 Introduction

SMT solvers [1] have enjoyed a recent widespread adoption to provide reasoning services in various applications, including interactive theorem provers like Isabelle [2], static checkers like Boogie [3], verification systems, e.g., ACL2 [4], Caduceus [5], software model checkers like SMT-CBMC [6], and unit test generators like CREST [7]. Research and development of SMT algorithms and tools is a very active research area, as witnessed by the annual competition, see e.g. [8]. It is fair to say that SMT solvers are the tool of choice in automated reasoning tasks involving Boolean combinations of constraints expressed in decidable background theories.

This paper is motivated by the fact that SMT solvers can also be used to solve formal verification problems involving neural networks [9]. Verification is indeed a standing challenge for neural networks which, in spite of some exceptions (see e.g., [10]), are confined to non-safety related equipment. The main reason is the lack of general, automated, yet effective safety assurance methods for neural-based systems, whereas existing mathematical methods require manual effort and ad-hoc arguments to justify safety claims [10].

In this paper we consider the problem of verifying a specific kind of neural network known as Multi-Layer Perceptron (MLP). The main feature of MLPs is that, even with a fairly simple topology, they can in principle approximate any non-linear mapping $f : \mathbb{R}^n \to \mathbb{R}^m$ with $n, m \geq 1$ – see [11]. We consider two different kinds of safety conditions. The first is checking that the output of an MLP always ranges within stated safety thresholds – a "global" safety bound. The second is checking that the output of an MLP is close to some kwown value or range of values modulo the expected error variance – a "local" safety bound. Both conditions can be tested by computing an abstraction, i.e., an overapproximation, of the concrete MLP and solving a satisfiability problem in Quantifier

* This research has received funding from the European Community's Information and Communication Technologies Seventh Framework Programme [FP7/2007-2013] under grant agreement N. 215805, the CHRIS project.

Free Linear Arithmetic over Reals (QF_LRA in [12]) using some SMT solver. Conservative abstraction guarantees that safety of the abstract MLP implies safety of the concrete one. On the other hand, realizable counterexamples demonstrate that the concrete MLP is unsafe, whereas spurious counterexamples call for a refinement of the abstraction.

The goal of this paper is to compare state-of-the-art SMT solvers on challenging test cases derived from verification problems involving MLPs – see Section 3. In particular, we consider HYSAT [13] a solver based on interval-arithmetic; MATHSAT [14], the winner of SMTCOMP 2010 in the QF_LRA category; and YICES [15] the winner of SMTCOMP 2009 in the same category. All the solvers above are tested extensively on different families of instances related to satisfiability checks in QF_LRA. These instances are obtained considering neural-based estimation of internal forces in the arm of a humanoid robot [16] – see Section 2. In particular, in Section 4 we describe three groups of experiments on the selected solvers. The first is a competition-style evaluation considering different safety flavours (local and global), different types and sizes of MLPs, and different degrees of abstraction "grain". The second is an analysis of scalability considering satisfiable and unsatisfiable encodings and varying the parameters which mostly influence performances in this regard. The last one is verification of the MLPs proposed in [16] with different solvers as back-ends. This experimental analysis shows that current state-of-the-art SMT solvers have the capability of attacking several non-trivial (sub)problems in the MLP verification arena. However, the overall verification process, particularly for networks of realistic size and fine grained abstractions, remains a standing open challenge.

2 Verification of MLPs: case study and basic concepts

All the encodings used in our analisys are obtained considering verification problems related to a control subsystem described in [16] to detect potentially unsafe situations in a humanoid robot. The idea is to detect contact with obstacles or humans, by measuring external forces using a single force/torque sensor placed along the kinematic chain of the arm. Measuring external forces requires *compensation* of the manipulator dynamic, i.e., the contribution of internal forces must be subtracted from sensor readings. Neural networks are a possible solution, but the actual network is to be considered safety-related equipment: An "incorrect" approximation of internal forces, may lead to either undercompensation – the robot is lured to believe that an obstacle exists – or overcompensation – the robot keeps moving even when an obstacle is hit. Internal forces estimation in [16] relies on a Multi-Layer Perceptron [17] (MLP). In the following, we introduce the main technical aspects of MLPs and their usage to estimate internal forces in James' arm.

MLPs are usually represented as a system of interconnected computing units (neurons), which are organized in layers. Figure 1 (left) shows an MLP consisting of three layers. The *input layer* serves to pass the input vector to the network, the *hidden layer* provides a first stage of computation, the *output layer* provides the final output. Operationally, MLPs implement the pseudo-code shown in Figure 1 (right). Given the network $\nu : \mathbb{R}^n \to \mathbb{R}^m$. The total input received by a neuron is called *induced local field* (ILF). With n neurons in the input layer and h neurons in the hidden layer the ILF of the j-th hidden neuron is defined as

$$r_j = \sum_{i=1}^{n} a_{ji} x_i + b_j \qquad j = \{1, \ldots, h\} \tag{1}$$

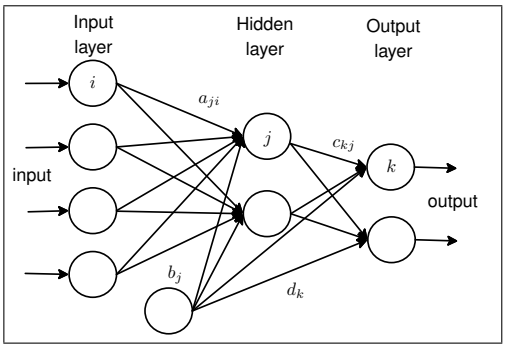


```
a[1,...,h][1,...,n] ▷ Input weights
c[1,...,m][1,...,h] ▷ Output weights
b[1,...,h]          ▷ Hidden nodes' bias
d[1,...,m]          ▷ Output nodes' bias

FUNCTION ν(x)
  for j ← 1 to h do
    r_j ← 0;
    for i ← 1 to n do
      r_j ← r_j + a_ji · x_i + b_j
  for k ← 1 to m do
    s_k ← 0;
    for j ← 1 to h do
      s_k ← s_k + c_kj · σ_h(r_j) + d_k
    y_k ← σ_o(s_k)
  return y
```

Fig. 1. Single hidden-layer MLP representations: graphical (left) and pseudo-code (right). In the graphical representation neurons and connections are represented by circles and arrows, respectively. In the pseudo-code, n, h and m are the numbers of input, hidden and output nodes, respectively; a,b,c and d are inductively synthesized numerical parameters; $\sigma_h : \mathbb{R} \to \mathbb{R}$ and $\sigma_o : \mathbb{R} \to \mathbb{R}$ are the functions computed in the hidden and output nodes, respectively; $\nu : \mathbb{R}^n \to \mathbb{R}^m$ is the function computed by the MLP.

where a_{ji} is the *weight* of the connection from the i-th neuron in the input layer to the j-th neuron in the hidden layer, and the constant b_j is the *bias* of the j-th neuron. The output of a neuron j in the hidden layer is a monotonic non-linear function of its ILF, the *activation function* σ_h. As long as the activation function is differentiable everywhere, MLPs with *only one* hidden layer can, in principle, approximate any real-valued function with n real-valued inputs [11]. Commonly used activation functions (see, e.g., [9]) are sigmoidal non-linearities such as the *hyperbolic tangent* (tanh) and the *logistic* (logi) functions defined as follows:

$$\tanh(r) = \frac{e^r - e^{-r}}{e^r + e^{-r}} \qquad \mathrm{logi}(r) = \frac{1}{1+e^{-r}} \tag{2}$$

where $\tanh : \mathbb{R} \to (-1, 1)$ and $\mathrm{logi} : \mathbb{R} \to (0, 1)$. The MLP suggested in [16] uses hyperbolic tangents, but our encodings are obtained using the logistic function instead.[1] With m neurons in the output layer the ILF of an output neuron is

$$s_k = \sum_{j=1}^{h} c_{kj}\sigma_h(r_j) + d_k \qquad k = \{1, \ldots, m\} \tag{3}$$

where c_{kj} denotes the weight of the connection from the j-th neuron in the hidden layer to the k-th neuron in the output layer, while d_k represents the bias of the k-th output neuron. Therefore, the output of the MLP is a vector $\nu(\underline{x}) = \{\sigma_o(s_1), \ldots, \sigma_o(s_m)\}$. The activation function σ_o can be either the identity function, i.e., $\nu(\underline{x}) = \{s_1, \ldots, s_m\}$, or a sigmoidal non-linearity as in (2). Notice that in the latter case, each output of ν is constrained to range within a known interval *by construction*. In applications where this is feasible, e.g., by rescaling input domains, this choice of σ effectively mitigates the risk of exceedingly low or high output values. In [16] tanh is used as activation funtion in the output neurons for this reason, and all inputs are rescaled in the range $[-1, 1]$.

[1] From a practical standpoint, the impact of our choice is negligible, since the logistic function has the same "shape" of the hyperbolic tangent, and they are often used interchangeably.

Using MLPs for estimation amounts to choose appropriate weights a, b, c and d. Technically, this is a *regression problem*, i.e., we are given a set of *patterns* – input vectors $X = \{\underline{x}_1, \ldots, \underline{x}_t\}$ with $\underline{x}_i \in \mathbb{R}^n$ – and a corresponding set of *labels* – output vectors $Y = \{\underline{y}_1, \ldots, \underline{y}_t\}$ with $\underline{y}_i \in \mathbb{R}^m$. We think of the labels as generated by some unknown function $\varphi : \mathbb{R}^n \to \mathbb{R}^m$ applied to the patterns, i.e., $\varphi(\underline{x}_i) = \underline{y}_i$ for $i \in \{1, \ldots, t\}$. The task of ν is thus to *extrapolate* φ, i.e., construct ν from X and Y so that given some $\underline{x}^* \notin X$ we ensure that $\nu(\underline{x}^*)$ is "as close as possible" to $\varphi(\underline{x}^*)$. In [16] internal forces in James' arm are estimated considering angular positions and velocities of two shoulder and two elbow joints, i.e., for each $\underline{x} \in X$, we have $\underline{x} = \langle q_1, \ldots, q_4, \dot{q}_1, \ldots, \dot{q}_4 \rangle$.[2] Labels $\underline{y} \in Y$ are corresponding values of internal forces and torques – denoted by f and τ, respectively – in a Cartesian space, i.e., $\underline{y} = \langle f_1, f_2, f_3, \tau_1, \tau_2, \tau_3 \rangle$. The unknown relation $\varphi : \mathbb{R}^8 \to \mathbb{R}^6$ is the one tying joint positions and velocities to internal forces, and takes into account components from gravity, Coriolis forces, and manipulator inertia.

Given a set of patterns X and a corresponding set of labels Y the process of tuning weights of an MLP ν in order to extrapolate φ – manipulator dynamic in our case – is called *training*, and the pair (X, Y) is called the *training set* – see [17] for details about the process. Even assuming that a training set is sufficient to learn φ, it is still the case that different sets may yield different MLP weights. The problem is that the resulting MLP may *underfit* the unknown target φ, i.e., consistently deviate from φ, or *overfit* φ, i.e., be very close to φ only when the input pattern is in the training set. These phenomena lead to poor *generalization* performances, i.e., the MLP largely fails to predict $\varphi(\underline{x}^*)$ on inputs $\underline{x}^* \notin X$. In our experiments, we use a *leave-one-out estimate* of the generalization error of an MLP as follows. Given the set (X, Y), the MLP $\nu_{(i)}$ is obtained by training on the patterns $X_{(i)} = \{x_1, \ldots, x_{i-1}, x_{i+1}, \ldots x_t\}$ and corresponding set labels $Y_{(i)}$. If we repeat the process t times, then we have t different MLPs and we obtain the estimate

$$\hat{\epsilon}_k = \frac{1}{t} \sum_{i=1}^{t} (\underline{y}_{ki} - \nu_{(i)}(\underline{x}_i))^2 \qquad k \in \{1, \ldots, m\} \tag{4}$$

where m is the number of outputs of each $\nu_{(i)}$. Notice that $\hat{\epsilon}_k$ is the mean squared error (MSE) among all the predictions made by each $\nu_{(i)}$ when tested on input $\underline{x}_i$. Clearly, $\hat{\underline{\epsilon}}$ should be kept at a minimum to ensure good generalization properties, but, as we show in the next Section, there is also an interplay between certain kinds of safety coditions and the standard deviation of $\hat{\underline{\epsilon}}$.

3 SMT encodings to verify MLPs

We consider two verification problems involving MLPs, and an approach to solve them using SMT encodings – more precisely, encodings in Quantifier Free Linear Arithmetic over Reals (QF_LRA) as defined in [12]. In the following we will always consider MLPs with $n \geq 1$ inputs and $m \geq 1$ outputs in which the *input domain* is a Cartesian product $\mathcal{I} = D_1 \times \ldots \times D_n$ where $D_i = [a_i, b_i]$ is a closed interval bounded by $a_i, b_i \in \mathbb{R}$ for all $1 \leq i \leq n$; analogously, the *output domain* is a Cartesian product $\mathcal{O} = E_1 \times \ldots \times E_m$ where $E_i = [c_i, d_i]$ is a closed interval bounded by $c_i, d_i \in \mathbb{R}$ for all $i \leq i \leq m$.[3]

[2] This is standard control-theory notation, where q represents the angular position of the joint, and $\dot{q}$ the angular velocity, i.e., the derivative of q with respect to time.

[3] In the definitions above, and throughout the rest of the paper, a closed interval $[a, b]$ bounded by $a, b \in \mathbb{R}$ is the set of real numbers comprised between a and b, i.e, $[a, b] = \{x \mid a \leq x \leq b\}$ with $a \leq b$.

3.1 Global safety

Checking for global safety of an MLP $\nu : \mathcal{I} \to \mathcal{O}$ amounts to prove that

$$\forall \underline{x} \in \mathcal{I}, \forall k \in \{1, \ldots, m\} : \nu_k(\underline{x}) \in [l_k, h_k] \tag{5}$$

where $\nu_k(\underline{x})$ denotes the k-th output of ν, and $l_k, h_k \in E_k$ are *safety thresholds*, i.e., constants defining an interval wherein the k-th component of the MLP output is to range, given all acceptable input values. Condition (5) can be checked on a *consistent abstraction* of ν, i.e., a function $\tilde{\nu}$ such that if the property corresponding to (5) is satisfied by $\tilde{\nu}$ in a suitable abstract domain, then it must hold also for ν. The key point is that verifying condition (5) in the abstract domain can be encoded to a satisfiability check in QF_LRA. Clearly, abstraction is not sufficient per se, because of *spurious counterexamples*, i.e., abstract counterexamples that do not correspond to concrete ones. A spurious counterexample calls for a refinement of the abstraction which, in turn, generates a new satisfiability check in QF_LRA. Therefore, a global safety check for a single output of ν may generate several logical queries to the underlying SMT solver. In practice, we hope to be able to either verify ν or exhibit a counterexample within a reasonable number of refinements.

In the following, we briefly sketch how to construct consistent abstractions and related refinements to check for property (5). Given a concrete domain $D = [a, b]$, the corresponding abstract domain is $[D] = \{[x, y] \mid a \leq x \leq y \leq b\}$, i.e., the set of intervals inside D, where $[x]$ is a generic element. We can naturally extend the abstraction to Cartesian products of domains, i.e., given $\mathcal{I} = D_1 \times \ldots \times D_n$, we define $[\mathcal{I}] = [D_1] \times \ldots \times [D_n]$, and we denote with $[\underline{x}] = \langle [x_1], \ldots, [x_n] \rangle$ the elements of $[\mathcal{I}]$ that we call *interval vectors*. Given a generic MLP ν – the *concrete* MLP – we construct the corresponding *abstract* MLP by assuming that σ_h is the logistic function logi : $\mathbb{R} \to (0, 1)$ as defined in (2), and that σ_o is the identity function. Since no ambiguity can arise between σ_h and σ_o, we denote σ_h with σ for the sake of simplicity. Given an abstraction parameter $p \in \mathbb{R}^+$, the *abstract activation function* $\tilde{\sigma}^p$ can be obtained by considering the maximum increment of σ over intervals of length p. Since σ is a monotonically increasing function, and the tangent to σ reaches a maximum slope of $1/4$ we have that

$$\forall x \in \mathbb{R} : 0 \leq \sigma(x + p) - \sigma(x) \leq \frac{p}{4} \tag{6}$$

for any choice of the parameter $p \in \mathbb{R}^+$. Now let x_0 and x_1 be the values that satisfy $\sigma(x_0) = p/4$ and $\sigma(x_1) = 1 - p/4$, respectively, and let $p \in (0, 1)$. We define $\tilde{\sigma}^p : [\mathbb{R}] \to [[0, 1]]$ as follows

$$\tilde{\sigma}^p([x_a, x_b]) = \begin{cases} [0, p/4] & \text{if } x_b \leq x_0 \\ [0, \sigma(\lfloor \frac{x_b}{p} \rfloor) + \frac{p}{4}] & \text{if } x_a \leq x_0 \text{ and } x_b < x_1 \\ [\sigma(\lfloor \frac{x_a}{p} \rfloor), \sigma(\lfloor \frac{x_b}{p} \rfloor) + \frac{p}{4}] & \text{if } x_0 < x_a \text{ and } x_b < x_1 \\ [\sigma(\lfloor \frac{x_a}{p} \rfloor), 1] & \text{if } x_0 < x_a \text{ and } x_1 \leq x_b \\ [1 - p/4, 1] & \text{if } x_a \geq x_1 \\ [0, 1] & \text{if } x_a \leq x_0 \text{ and } x_1 \leq x_b \end{cases} \tag{7}$$

Figure 2 gives a pictorial representation of the above definition.

According to (7) we can control how much $\tilde{\sigma}^p$ over-approximates σ, since large values of p correspond to coarse-grained abstractions, whereas small values of p correspond to fine-grained ones. We can now define $\tilde{\nu}^p : [\mathcal{I}] \to [\mathcal{O}]$ as

$$\tilde{\nu}^p_k([\underline{x}]) = \sum_{j=1}^{h} c_{kj} \tilde{\sigma}^p(\tilde{r}_j([\underline{x}])) + d_k \qquad k = \{1, \ldots, m\} \tag{8}$$

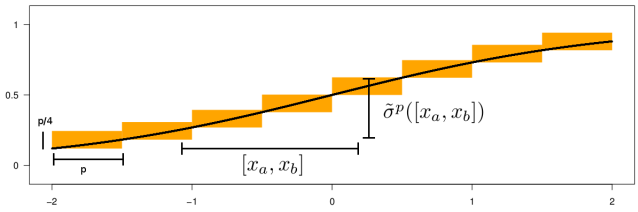

Fig. 2. Activation function $\sigma(x)$ and its abstraction $\tilde{\sigma}^p(x)$ in the range $x \in [-2, 2]$. The solid line denotes σ, while the boxes denote $\tilde{\sigma}^p$ with $p = 0.5$.

where $\tilde{r}_j([\underline{x}]) = \sum_{i=1}^{n} a_{ji}[x_i] + b_j$ for all $j = \{1, \ldots, h\}$, and we overload the standard symbols to denote products and sums among interval vectors, e.g., we write $x + y$ to mean $x \tilde{+} y$ when $x, y \in [\mathbb{R}]$. Since $\tilde{\sigma}^p$ is a consistent abstraction of σ, and products and sums on intervals are consistent abstractions of the corresponding operations on real numbers, defining $\tilde{\nu}^p$ as in (8) provides a consistent abstraction of ν. This means that our original goal of proving the safety of ν according to (5) can be now recast, modulo refinements, to the goal of proving its abstract counterpart

$$\forall [\underline{x}] \in [\mathcal{I}], \forall k \in \{1, \ldots, m\} : \tilde{\nu}_k^p([\underline{x}]) \sqsubseteq [l_k, h_k] \tag{9}$$

where "$\sqsubseteq$" stands for the usual containment relation between intervals, i.e., given two intervals $[a, b] \in [\mathbb{R}]$ and $[c, d] \in [\mathbb{R}]$ we have that $[a, b] \sqsubseteq [c, d]$ exactly when $a \geq c$ and $b \leq d$, i.e., $[a, b]$ is a subinterval of – or it coincides with – $[c, d]$.

3.2 Local safety

The need to check for global safety can be mitigated using sigmoidal non-linearities in the output neurons to "squash" the response of the MLP within an acceptable range, modulo rescaling. A more stringent, yet necessary, requirement is reprensented by local safety. Informally speaking, we can say that an MLP ν trained on a dataset (X, Y) of t patterns is "locally safe" whenever given an input pattern $\underline{x}^*$ it turns out that $\nu(\underline{x}^*)$ is "close" to $\underline{y}_j \in Y$ as long as $\underline{x}^*$ is "close" to $\underline{x}_j \in X$ for some $j \in \{1, \ldots, t\}$. Local safety cannot be guaranteed by design, because the range of acceptable values varies from point to point. Moreover, it ensures that the error of an MLP never exceeds a given bound on yet-to-be-seen inputs, and it ensures that the response of an MLP is relatively stable with respect to small perturbations in its input.

To formalize local safety, given an MLP $\nu : \mathcal{I} \to \mathcal{O}$, and a training set (X, Y) consisting of t elements, we introduced the following concepts. Given two patterns $\underline{x}, \underline{x}' \in X$ their *distance along the i-th dimension* is defined as $\delta_i(\underline{x}, \underline{x}') = |x_i' - x_i|$. Given some $\underline{x} \in X$, the function $N_i^q : X \to 2^X$ maps $\underline{x}$ to the set of *q-nearest-neighbours along the i-th dimension*, i.e., the first q elements of the list $\{\underline{x}' \in X \mid \underline{x}' \neq \underline{x}\}$ sorted in ascending order according to $\delta_i(\underline{x}, \underline{x}')$. Given some $\underline{x} \in X$, the function $\delta_i^q : X \to \mathbb{R}$ maps $\underline{x}$ to the *q-nearest-distance along the i-th dimension*, i.e.,

$$\delta_i^q(\underline{x}) = \max_{\underline{x}' \in N_i^q(\underline{x})} \delta_i(\underline{x}, \underline{x}')$$

The q-n-*polytope* $\mathcal{X}_j^q$ corresponding to $\underline{x}_j \in X$ for some $j \in \{1, \ldots, t\}$ is the region of space comprised within all the $2n$ hyper-planes obtained by considering, for each dimension i, the two hyper-planes perpendicular to the i-th axis and intersecting it in $(x_i - \delta_i^q(\underline{x}))$ and $(x_i + \delta_i^q(\underline{x}))$, respectively. The above definitions can be repeated for labels, and thus $\mathcal{Y}_j^q$ denotes a q-m-polytope associated to $\underline{y}_j \in Y$ for some $j \in \{1, \ldots, t\}$. In the following, when the dimensionality is understood from the context, we use $\mathcal{X}$ to denote 1-n-polytopes, and $\mathcal{Y}$ to denote 1-m-polytopes. In the following, we refer to q as the *neighborhood size*.

Given an MLP $\nu : \mathcal{I} \to \mathcal{O}$ with training set (X, Y) consisting of t patterns we consider, for all $j \in \{1, \ldots, t\}$, the set of *input polytopes* $\{\mathcal{X}_1, \ldots, \mathcal{X}_t\}$ associated with each pattern $\underline{x}_j \in X$, and the set of *output polytopes* $\{\mathcal{Y}_1^q, \ldots, \mathcal{Y}_t^q\}$ associated with each label $\underline{y}_j \in Y$, for a fixed value of q. We say that ν is locally safe if the following condition is satisfied

$$\forall \underline{x}^* \in \mathcal{I}, \exists j \in \{1, \ldots, t\} : \underline{x}^* \in \mathcal{X}_j \to \underline{\nu}(\underline{x}^*) \in \mathcal{Y}_j^q \tag{10}$$

Notice that this condition is trivially satisfied by all the input patterns $\underline{x}^*$ such that $\underline{x}^* \in \mathcal{I}$ but $\underline{x}^* \notin \mathcal{X}_j$ for all $j \in \{1, \ldots, t\}$. Indeed, these are patterns which are "too far" from known patterns in the training set, and for which we simply do not have enough information in terms of local (un)safety. Also, we always consider 1-n-polytopes on the input side of ν whereas we can vary the size of neighbourhoods on the output side by increasing q. Clearly, the larger is q, the larger is the neighbourhood considered in the output, and the less stringent condition (10) becomes. This additional degree of freedom is important in order to "tune" the safety condition according to the expected variance in the network error. Intuitively, assuming that we obtained a network whose expected error mean and variance is satisfactory, if we try to certify such network on safety bounds which imply a smaller error variance, we will invariably generate feasible counterexamples. The abstraction-refinement approach to check local safety is similar to the one described for global safety. In particular, the abstract network $\tilde{\nu}^p$ is obtained as shown previously, i.e., by abstracting the activation function and thus the whole network to compute interval vectors. The abstract local safety condition corresponding to (10), for any fixed value of k, is

$$\forall [\underline{x}^*] \in [\mathcal{I}], \exists i \in \{1, \ldots, t\} : [\underline{x}^*] \in \mathcal{X}_i \to \tilde{\nu}([\underline{x}^*]) \sqsubseteq \mathcal{Y}_i^k \tag{11}$$

It can be shown that the above condition implies local safety of the concrete network ν, and, as in the case of (9), verifying it can be encoded into a QF_LRA satisfiability check.

4 Challenging SMT solvers to verify MLPs

The experiments detailed in this section are carried out on a family of identical Linux workstations comprised of 10 Intel Core 2 Duo 2.13 GHz PCs with 4GB of RAM. Unless otherwise specified, the resources granted to the solvers are 600s of CPU time and 2GB of memory. The solvers involved in the evaluation are CVC [18] (version 3.2.3, default options), HYSAT [13] (version 0.8.6, $\varepsilon = 10^{-5}$ and $\delta = 10^6$ options), MATHSAT [14] (version 4, `-no_random_decisions` option), and YICES [15] (version 2, default options).

To compare the solvers we use encodings considering both global and local safety, different types and sizes of MLPs, and different degrees of abstraction grain. We classify the encodings in "Suites" and "Families". The former distinction is about global vs. local safety, from which we obtain two suites, namely GLOBAL and LOCAL. For each suite, we

Solver	Total		Sat		Unsat	
	#	Time	#	Time	#	Time
YICES	809	27531.90	639	22141.03	170	5390.87
HYSAT	698	17641.61	561	13089.82	137	4551.79
MATHSAT	683	41975.01	544	35043.15	139	6931.86
CVC	–	–	–	–	–	–

Table 1. Evaluation results at a glance. We report the number of encodings solved within the time limit ("#") and the total CPU time ("Time") spend on the solved encodings. Total number of formulas solved ("Total") is also split in satisfiable and unsatisfiable formulas ("Sat") and ("Unsat"), respectively. Solvers are sorted according to the number of encodings solved. A dash means that a solver did not solve any encoding in the related group.

group encodings in families differing for the number of hidden neurons and the numbers of output neurons. The family HN-XX_ON-YY denotes encodings with XX hidden and YY output neurons, respectively. We vary the number of hidden neurons in the range $\{5, 10, 20\}$ and we consider either one or six output neurons. For each suite, we produce all possible encodings obtained combining different values of these parameters. Finally, for each family, we encode formulas from $p = 0.5$, and decreasing it by a rate $r = 1.3$, i.e., $p = p/r$ at each refinement step. We stop when we obtain 20 encodings for each family. Moreover, in the case of LOCAL, we compute encodings with different neighborhood sizes, i.e. $q = \{1, 10, 20, 50, 100, 199\}$.

In Table 1 we report a global picture of the evaluation results. In the following, when we say that "solver A *dominates* solver B" we mean that the set of problems solved by B is a subset of those solved by A. Looking at the result, we can see that all solvers but CVC, were able to solve at least 70% of the test set. CVC exhausts memory resources before reaching the time limit, and it is able to solve no encodings, thus we drop it from the analysis. Still looking at Table 1, we can see that YICES outperforms the other solvers conquering 96% of the test set, while HYSAT and MATHSAT were able to solve 83% and 81%, respectively. Despite the very similar performance of HYSAT and MATHSAT – only 15 encodings separate them – we can see that HYSAT spends about 42% of the CPU time spent by MATHSAT. We also report that HYSAT, has the best average time per encoding (about 25s) with respect to both YICES (about 34s) and MATHSAT (about 61s). Finally, we report no discrepancies in the satisfiability result of the evaluated solvers.

Table 2 shows the results of the evaluation dividing the encodings by suites and families. As we can see, in terms of number of encodings solved, YICES is the strongest solver. Concerning the suite GLOBAL, it leads the count with 109 solved encoding (91% of the test set), while concerning the LOCAL suite, it solves 700 encodings (97% of the test set). Focusing on the suite GLOBAL, 10 encodings separate the strongest solver from the weakest one – HYSAT, that solves 99 encodings (82% of the test set). If we consider the problems that are uniquely solved, then we see that no solver is dominated by the others. Now focusing on the suite LOCAL, the first thing to observe is that the difference between the strongest and the weakest solver is increased: 101 encodings separate YICES and MATHSAT, the was able to solve 580 encodings (about 80% of the test set). We also report that MATHSAT is dominated by YICES.

In Table 3 we show the classification of encodings included in the test set. In the table, the number of encodings solved and the cumulative time taken for each family

Suite	Family	Solver	Total		Sat		Unsat		Unique	
			#	Time	#	Time	#	Time	#	Time
GLOBAL (120)	HN-5_ON-1 (20)	YICES	20	23.889	20	23.889	–	–	–	–
		MATHSAT	20	281.56	20	281.56	–	–	–	–
		HYSAT	12	288.91	12	288.91	–	–	–	–
	HN-5_ON-6 (20)	YICES	20	28.90	20	28.90	–	–	–	–
		HYSAT	20	712.30	20	712.30	–	–	–	–
		MATHSAT	19	548.96	19	548.96	–	–	–	–
	HN-10_ON-1 (20)	YICES	19	493.71	19	493.701	–	–	3	115.68
		HYSAT	17	816.59	17	816.59	–	–	1	478.53
		MATHSAT	9	731.21	9	731.21	–	–	–	–
	HN-10_ON-6 (20)	HYSAT	19	902.85	19	902.85	–	–	1	4.68
		YICES	19	1188.10	19	1188.10	–	–	–	–
		MATHSAT	15	1112.26	15	1112.26	–	–	–	–
	HN-20_ON-1 (20)	MATHSAT	20	1178.47	20	1178.47	–	–	2	326.58
		YICES	18	1637.82	18	1637.82	–	–	–	–
		HYSAT	17	1066.20	17	1066.20	–	–	–	–
	HN-20_ON-6 (20)	MATHSAT	20	1034.77	20	1034.77	–	–	2	406.29
		HYSAT	14	961.40	14	961.40	–	–	–	–
		YICES	13	2633.74	13	2633.74	–	–	–	–
LOCAL (720)	HN-5_ON-1 (120)	YICES	120	910.77	82	451.68	38	459.09	13	592.63
		MATHSAT	106	5103.72	74	2860.42	32	2243.30	–	–
		HYSAT	98	1639.34	70	393.22	28	1246.11	–	–
	HN-5_ON-6 (120)	HYSAT	120	20.57	100	19.53	20	1.04	–	–
		YICES	120	1225.49	100	1134.06	20	91.43	–	–
		MATHSAT	113	4714.75	93	4272.69	20	442.06	–	–
	HN-10_ON-1 (120)	YICES	120	2808.87	83	1603.70	37	1205.17	22	2194.79
		HYSAT	94	5382.65	67	3469.57	27	1913.08	–	–
		MATHSAT	94	6802.15	67	4412.35	27	2389.80	–	–
	HN-10_ON-6 (120)	YICES	120	4047.18	100	3760.97	20	286.20	9	1729.51
		HYSAT	106	1346.47	86	1344.97	20	1.49	–	–
		MATHSAT	104	6272.87	84	5728.48	20	544.39	–	–
	HN-20_ON-1 (120)	YICES	115	6014.31	80	3563.78	35	2450.53	23	4274.22
		HYSAT	90	2651.61	67	1263.40	23	1388.22	–	–
		MATHSAT	76	6420.13	56	5796.93	20	623.19	–	–
	HN-20_ON-6 (120)	YICES	105	6519.13	85	5620.70	20	898.43	11	3238.09
		HYSAT	91	1852.71	72	1850.86	19	1.85	1	3.03
		MATHSAT	87	7774.15	67	7085.04	20	689.11	–	–

Table 2. Solver-centric view of the results. Columns "Suite" and "Family" report suite and family name of the encodings, respectively. The remainder of the table is organized similarly to Table 1, with the exception of column ("Unique"), that shows data about uniquely solved encodings.

Family	Overall		Time	Hardness			Family	Overall		Time	Hardness		
	N	#		EA	ME	MH		N	#		EA	ME	MH
GLOBAL_HN-5_ON-1	20	20	23.89	12	8	–	LOCAL_HN-5_ON-1	120	120	823.53	97	10	13
GLOBAL_HN-5_ON-6	20	20	28.91	19	1	–	LOCAL_HN-5_ON-6	120	120	20.57	113	7	–
GLOBAL_HN-10_ON-1	20	20	744.19	9	7	4	LOCAL_HN-10_ON-1	120	120	2563.94	90	8	22
GLOBAL_HN-10_ON-6	20	20	345.42	14	5	1	LOCAL_HN-10_ON-6	120	120	2137.99	99	12	9
GLOBAL_HN-20_ON-1	20	20	906.36	17	1	2	LOCAL_HN-20_ON-1	120	115	4811.98	74	18	23
GLOBAL_HN-20_ON-6	20	20	827.05	9	9	2	LOCAL_HN-20_ON-6	120	106	4484.83	83	11	12

Table 3. Encoding-centric view of the results. The table consists of seven columns where for each family of encodings we report the name of the family in alphabetical order (column "Family"), the number of encodings included in the family, and the number of encodings solved (group "Overall", columns "N", "#", respectively), the CPU time taken to solve the encodings (column "Time"), the number of easy, medium and medium-hard encodings (group "Hardness", columns "EA", "ME", "MH").

is computed considering the "SOTA solver", i.e., the ideal solver that always fares the best time among all considered solvers. An encoding is thus solved if at least one of

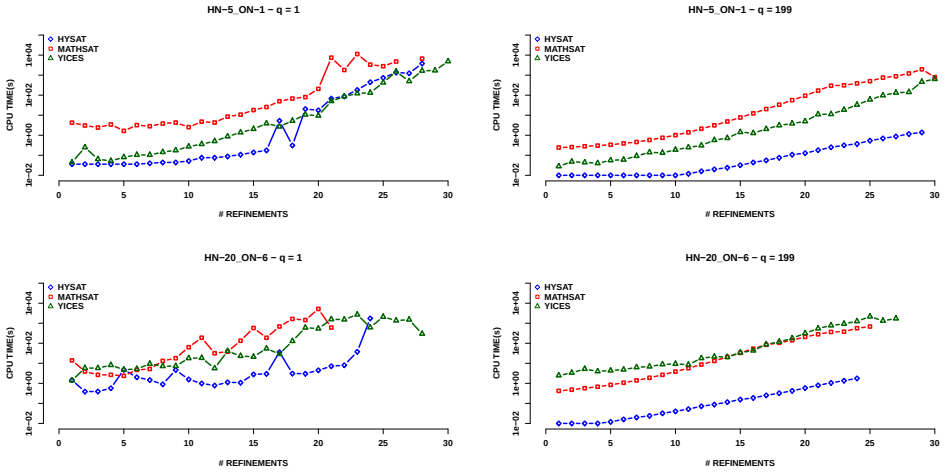

Fig. 3. Scalability test on the evaluated solvers. For each plot, in x axis is shown the refinement step, while in the y axis (in logarithmic scale) the related CPU time (in seconds). HYSAT performance is depicted by blue diamonds, while MATHSAT and YICES results are denoted by red boxes and green triangles, respectively. Plots in the same column are related to encodings having tha same satisfiability result, i.e. SAT (left-most column) and UNSAT (right-most column). Plots in the same row are related to encodings having tha same MLP architecture, i.e. HN-5_ON-1 (top) and HN-20_ON-6 (bottom).

the solvers solves it, and the time taken is the best among all times of the solvers that solved the encoding. The encodings are classified according to their hardness with the following criteria: easy encodings are those solved by all the solvers, medium encodings are those non easy encodings that could still be solved by at least two solvers, medium-hard encodings are those solved by one reasoner only, and hard encodings are those that remained unsolved.

According to the data summarized in Table 3, the test set consisted in 840 encodings, 821 of which have been solved, resulting in 636 easy, 97 medium, 88 medium-hard, and 19 hard encodings. Focusing on families comprised in the suite GLOBAL, we report that all 120 encodings were solved, resulting in 80 easy, 31 medium, and 9 medium-hard encodings. Considering the families in LOCAL, we report that 821 encodings (out of 840) were solved, resulting in 636 easy, 97 medium, and 88 medium-hard encodings.

Finally, we report the contribution of each solver to the composition of the SOTA solver. Focusing on the suite GLOBAL, YICES contributed to the SOTA solver 77 times (out of 120), while MATHSAT and HYSAT 29 and 14 times, respectively. If we consider now the suite LOCAL, the picture is quite different: HYSAT contributed 509 times, while YICES and MATHSAT 188 and 4 times, respectively. Considering all 821 solved encodings, we report that HYSAT was the main contributor (64%), despite the fact that it is not the best solver in terms of total amount of solved encodings.

Our next experiment aims to draw some conclusions about the scalability of the evaluated solvers. In order to do that, we compute a pool of encodings satisying the following desiderata:

1. Consider values of the abstraction parameter p which correspond to increasingly fine-grained abstractions.
2. Consider different MLP size in terms of hidden neurons.
3. Consider the satisfiability result of the computed encodings.

To cope with (1), we generate encodings related to 30 refinement steps. To take care the potentially increasing difficulty of such encodings, we set the time limit to 4 CPU hours. In order to satisfy desideratan (2), we compute encodings both considering HN-5_ON-1 and HN-20_ON-6 MLP architectures. Finally, in order to cover (3), we focus on the suite LOCAL, selecting the encodings related to $q = 1$, and $q = 199$. The former encodings are almost always satisfiable, i.e., an abstract counterexamples is easily found, and, conversely, the latter encodings are almost always unsatisfiable.

As a result of the selection above, we obtain 4 groups of encodings, and Figure 3 shows the results of experimenting with them. Looking at Figure 3 (top-left), we can see that HYSAT is the best solver along the first 17 refinement steps. After this point, its performance is comparable to YICES, but with the noticeable difference that the latter is able to solve all the encodings, while HYSAT exhausts CPU time resources trying to solve the two encodings having the smallest value of p. The CPU time spent by MATHSATon each of the first 24 refinement steps is at least one order of magnitude higher than HYSAT and YICES. Considering now the same safety problem, but related to a larger MLP architecture, we can see a different picture. From Figure 3 (bottom-left), we can see that no solver is able to solve all the encodings within 4 CPU hours. In particular, MATHSAT stops at the 21st step (out of 30), while YICES is able to solve all encodings but the last two. While the performances of MATHSAT and YICES seems to have a smooth increasing trend, HYSAT is less predictable: In the first 22 refinement steps it is up to one order of magnitude faster than YICES– with the noticeable exception of four "peaks" – and for the following two steps it is two order of magnitude slower than YICES.

Considering now the plots in Figure 3 (right), we can see that the trend in solver's performance is much smoother than the plots in Figure 3 (left). Looking at Figure 3 (top-right), we can see that, excluding the last encoding, HYSAT is one order of magnitude faster than YICES, that in turn is one order of magnitude faster that MATHSAT. Looking now at the last plot, we can see that we have to main differences with respect to the picture resulting from the previous plot. First, the encodings are more challenging, because no solver was able to solve all the pool within the CPU time limit. Second, there is no noticeable difference – excluding the last two solved encodings – between MATHSAT and YICES.

Our last experiment concerns the analysis of various solvers as back-ends. We experiment with a local safety problem with $k = 75$, $p = 0.5$, and $r = 1.1$ about an MLP having a HN-20_ON-6 architecture. In Figure 4 we report the results of such experiment. Also if we are not able to conclude about the safety of the considered MLP because all solvers exhaust their memory resources, looking at the figure we can see that YICES clearly outperforms both MATHSAT and HYSAT. YICES enabled allowed to refine 54 times, while MATHSAT and HYSAT stopped to 32 and 21 refinements, respectively. Concerning the cumulative CPU time, performances of MATHSAT and YICES are in the same ballpark until the 12th step, and they increase smoothly until the end of the computation. On the other hand, if we look at HYSAT performance, we can see that it is very close to be constant, with the noticeable exception of two peaks: The first one (between step 3 and 4) is small, and the second one (between step 9 and 10) implies a two orders of magnitude jump in

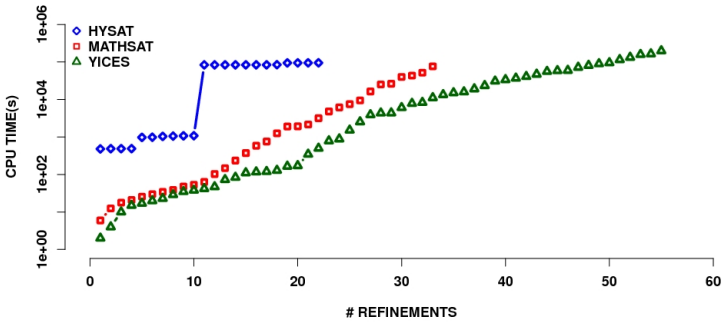

Fig. 4. CPU cumulative time (y axis) vs. number of refinement steps (x axis) with different back-engines. The plot is organized similarly to the plots in Figure 3.

the cumulative CPU time. In this problem, HYSAT shows the same behaviour shown in Figure 3 (bottom-left).

References

1. C. Barrett, R. Sebastiani, S.A. Seshia, and C. Tinelli. Satisfiability modulo theories. *Handbook of Satisfiability, IOS Press, Amsterdam*, pages 825–885, 2009.
2. P. Fontaine, J.Y. Marion, S. Merz, L. Nieto, and A. Tiu. Expressiveness+ automation+ soundness: Towards combining SMT solvers and interactive proof assistants. *Tools and Algorithms for the Construction and Analysis of Systems*, pages 167–181, 2006.
3. R. DeLine and K.R.M. Leino. BoogiePL: A typed procedural language for checking object-oriented programs. 2005.
4. S. Ray. Connecting External Deduction Tools with ACL2. *Scalable Techniques for Formal Verification*, pages 195–216, 2010.
5. J.C. Filliâtre and C. Marché. The Why/Krakatoa/Caduceus platform for deductive program verification. In *Proceedings of the 19th international conference on Computer aided verification*, pages 173–177. Springer-Verlag, 2007.
6. A. Armando, J. Mantovani, and L. Platania. Bounded model checking of software using SMT solvers instead of SAT solvers. *International Journal on Software Tools for Technology Transfer (STTT)*, 11(1):69–83, 2009.
7. T.A. Hoang and N.N. Binh. Extending CREST with Multiple SMT Solvers and Real Arithmetic. In *Knowledge and Systems Engineering (KSE), 2010 Second International Conference on*, pages 183–187. IEEE.
8. C. Barrett, L. de Moura, and A. Stump. SMT-COMP: Satisfiability Modulo Theories Competition. In K. Etessami and S. Rajamani, editors, *17th International Conference on Computer Aided Verification*, pages 20–23. Springer, 2005.
9. C.M. Bishop. Neural networks and their applications. *Review of scientific instruments*, 65(6):1803–1832, 2009.
10. J. Schumann and Y. Liu, editors. *Applications of Neural Networks in High Assurance Systems*, volume 268 of *Studies in Computational Intelligence*. Springer, 2010.
11. K. Hornik, M. Stinchcombe, and H. White. Multilayer feedforward networks are universal approximators. *Neural networks*, 2(5):359–366, 1989.
12. D.R. Cok. The SMT-LIBv2 Language and Tools: A Tutorial, 2011. Available from `http://www.grammatech.com/resources/smt/`.
13. M. Franzle, C. Herde, T. Teige, S. Ratschan, and T. Schubert. Efficient solving of large non-linear arithmetic constraint systems with complex boolean structure. *Journal on Satisfiability, Boolean Modeling and Computation*, 1:209–236, 2007.
14. R. Bruttomesso, A. Cimatti, A. Franzén, A. Griggio, and R. Sebastiani. The MathSAT 4 SMT Solver. In *Proceedings of the 20th international conference on Computer Aided Verification*, pages 299–303. Springer-Verlag, 2008.
15. B. Dutertre and L. De Moura. A fast linear-arithmetic solver for DPLL (T). In *Computer Aided Verification*, pages 81–94. Springer, 2006.
16. M. Fumagalli, A. Gijsberts, S. Ivaldi, L. Jamone, G. Metta, L. Natale, F. Nori, and G. Sandini. Learning to Exploit Proximal Force Sensing: a Comparison Approach. *From Motor Learning to Interaction Learning in Robots*, pages 149–167, 2010.
17. S. Haykin. *Neural networks: a comprehensive foundation*. Prentice Hall, 2008.
18. C. Barrett and C. Tinelli. CVC3. In *Proceedings of the 19th International Conference on Computer Aided Verification (CAV'07)*, volume 4590 of *Lecture Notes in Computer Science*, pages 298–302. Springer-Verlag, 2007.